Targeting Alzheimer amyloid plaques in vivo

Thomas M. Wengenack, Geoffry L. Curran, and Joseph F. Poduslo*

Molecular Neurobiology Laboratory, Departments of Neurology and Biochemistry/Molecular Biology, Mayo Clinic and Foundation, Rochester, MN 55905. Corresponding author (poduslo.joseph@mayo.edu).

Received 31 January 2000; accepted 30 May 2000

The only definitive diagnosis for Alzheimer disease (AD) at present is postmortem observation of neuritic plaques and neurofibrillary tangles in brain sections. Radiolabeled amyloid-β peptide (Aβ), which has been shown to label neuritic plaques in vitro, therefore could provide a diagnostic tool if it also labels neuritic plaques in vivo following intravenous injection. In this study, we show that the permeability of Aβ at the blood–brain barrier can be increased by at least twofold through covalent modification with the naturally occurring polyamine, putrescine. We also show that, following intravenous injection, radiolabeled, putrescine-modified Aβ labels amyloid deposits in vivo in a transgenic mouse model of AD, as well as in vitro in human AD brain sections. This technology, when applied to humans, may be used to detect plaques in vivo, allowing early diagnosis of the disease and therapeutic intervention before cognitive decline occurs.

Keywords: Alzheimer disease, amyloid, labeling, imaging, diagnosis, transgenic

Early diagnosis of Alzheimer disease (AD) is prevented by the inability to visualize plaques in the brain. Alzheimer disease is characterized by neuritic plaques and neurofibrillary tangles. Neuritic, or senile plaques contain a dense core consisting largely of several species of amyloid-β (Aβ), a highly hydrophobic peptide that spontaneously aggregates in vitro[1] and has been reported to be neurotoxic in vitro[2] and in vivo[3]. The main link between AD and Aβ is based on genetic mutations that have been discovered in familial forms of AD and Down syndrome that result in increased levels and deposition of Aβ[4]. Furthermore, transgenic mice overexpressing the same mutations have been shown to develop amyloid deposits like those in AD as well as behavioral deficits[5,6]. Additionally, one study has reported a significant correlation between amyloid burden and dementia in AD patients[7].

Currently, there is no definitive diagnosis for AD except by postmortem observation of plaques and tangles and by eliminating other neurodegenerative disorders. It has been observed that ^{125}I-radiolabeled Aβ 1-40 binds to aggregated Aβ in vitro[8], and binds to and labels dense-core, neuritic-type, but not diffuse plaques in AD brain sections in vitro[8]. Therefore, radiolabeled Aβ 1-40 when injected intravenously might also label neuritic plaques in vivo and, with the appropriate radioisotope, be used as a probe for measuring amyloid burden, thereby providing a more definitive premortem diagnosis of AD in humans. In one experiment using aged squirrel monkeys exhibiting amyloid deposits with advanced age, amyloid deposits in brain were labeled following injection of radiolabeled Aβ 1-40 into the carotid artery, but only in cerebrovascular amyloid deposits[9]. Transgenic mice expressing both mutant human amyloid precursor protein (APP) and presenilin 1 (PS1) exhibit abundant neuritic-type amyloid deposits and behavioral deficits in as little as 12 weeks[6] and may provide a more suitable model to test this hypothesis.

Techniques have been developed to measure the permeability of peptides and proteins at the blood–brain barrier (BBB)[10-12], and to increase that permeability, through covalent modification with such naturally occurring polyamines as putrescine, spermidine, or spermine[13–16]. The use of a labeled peptide with greater permeability at the BBB might increase sensitivity and allow the use of lower quantities of radioisotope. This would be of considerable value since these techniques would ultimately be used in humans.

The purpose of the present study was to determine if radiolabeled, putrescine-modified Aβ 1-40 would label amyloid deposits in vivo following intravenous injection in a transgenic mouse model of AD. Initial experiments were performed to measure the BBB permeabilities of native and putrescine-modified Aβ 1-40, as well as to compare the ability of radioiodinated native and putrescine-modified Aβ 1-40 to label amyloid deposits in AD brain in vitro. Our studies show that we can radiolabel neuritic plaques in vivo in a transgenic mouse model of AD. The next step is to apply our technology to human disease for early diagnosis of the disease and therapeutic intervention.

Results

BBB permeability of putrescine-modified Aβ 1-40. Putrescine-modified Aβ 1-40 (PUT-Aβ 1-40) exhibits increased permeability at the BBB compared to native Aβ 1-40, as determined by intravenous bolus injection technique[10–12]. Putrescine modification significantly increased the BBB permeability of PUT-Aβ 1-40 in all brain regions measured, compared to Aβ 1-40, with significant increases in the product of permeability coefficient × surface area (PS), ranging from 1.9-fold in the hippocampus to 2.3-fold in the cortex (Table 1). The residual plasma volume (V_p) was increased slightly but significantly in three of six brain regions (Table 1). This was probably a result of the large increases in the PS values observed for PUT-Aβ 1-40, with some of the peptide crossing the BBB even during the 15 s period taken for the administration of the second isotope.

Labeling of amyloid plaques in vitro. The next step was to determine if PUT-Aβ 1-40 can bind and label amyloid deposits in AD brain sections in vitro as reported for Aβ 1-40 (ref. 8). Aβ 1-40 and PUT-Aβ 1-40 were first radiolabeled with ^{125}I to facilitate detection and then purified by reversed-phase high-performance liquid chromatography (RP-HPLC) to remove unbound ^{125}I and unlabeled peptide. Chromatograms of HPLC elution profiles of unlabeled Aβ 1-40 and PUT-Aβ 1-40 are shown in Figure 1. Because the positively charged amine groups of putrescine make PUT-Aβ 1-40 less

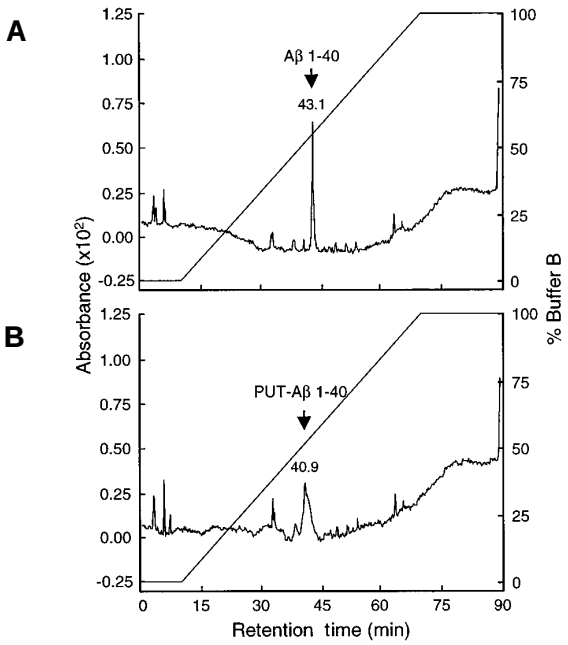

Figure 1. RP-HPLC chromatograms of unlabeled Aβ 1-40 (A) and PUT-Aβ 1-40 (B). The abscissa plots the retention time in minutes. The left ordinate plots the absorbance at 214 nm. The right ordinate plots the gradient as percentage of buffer B (80% ACN, 0.05% TFA, 19.95% HPLC water).

hydrophobic, it elutes earlier than Aβ 1-40. HPLC-purified ^{125}I-Aβ 1-40 and ^{125}I-PUT-Aβ 1-40 were incubated with adjacent sections of unfixed AD temporal lobe cortex. Following immunohistochemical analysis (IH) to visualize the amyloid deposits, we exposed the sections first to film and then emulsion autoradiography to detect the presence of the ^{125}I-Aβ 1-40 or ^{125}I-PUT-Aβ 1-40. The X-ray film (Fig. 2) demonstrates the presence of punctate areas of exposed film located predominantly in the regions corresponding to gray matter. This is similar to the distribution of amyloid deposits seen following IH of the tissue sections. It was possible to overlay the two for direct comparison under the microscope (data not shown). A longer duration of exposure was required for ^{125}I-Aβ 1-40 (six days) to achieve a relative intensity equal to that of ^{125}I-PUT-Aβ 1-40 (one day), suggesting that ^{125}I-PUT-Aβ 1-40 may have greater affinity to the amyloid deposits than ^{125}I-Aβ 1-40.

In order to directly correlate the IH with the iodinated peptide by colocalization, the sections were next dipped in an autoradiographic emulsion to detect the iodinated peptide as revealed by exposed (blackened) silver grains directly on the same tissue previously stained with anti-Aβ antibody. These results are illustrated in photomicrographs Figures 3 and 4. Figure 3 illustrates the in vitro binding of equal amounts of radioactivity of ^{125}I-Aβ 1-40 and ^{125}I-PUT-Aβ 1-40 to amyloid deposits in adjacent sections of AD temporal lobe cortex. All sections were processed for anti-Aβ IH and emulsion autoradiography with an equal exposure time of six days. The amyloid deposits appear brown. The presence of iodinated peptide is indicated by increased density of black, exposed silver grains. The specificity of binding of both peptides to the amyloid deposits is demonstrated by the low density of exposed silver grains in the background. Furthermore, binding seems to be more selective for the dense-core, neuritic-type plaques on the left than for the diffuse plaque located on the right (Fig. 3E, F). Also, with equal amounts of radioactivity and exposure time, the higher density of silver grains for ^{125}I-PUT-Aβ 1-40 suggests that the modified peptide has a greater affinity for the neuritic plaques than does ^{125}I-Aβ 1-40. Binding of equal peptide concentrations of ^{125}I-Aβ 1-40 and ^{125}I-PUT-Aβ 1-40 to amyloid deposits in vitro yielded results similar to Figure 3 (data not shown).

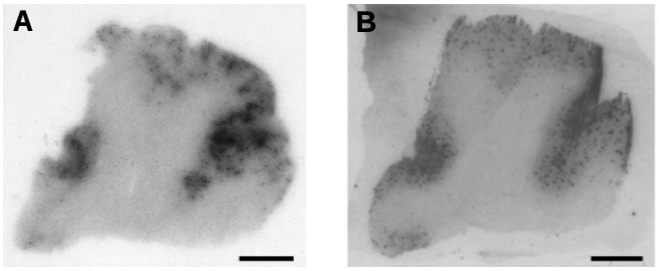

Figure 2. ^{125}I-Aβ 1-40 and ^{125}I-PUT-Aβ 1-40 labeling of amyloid deposits in vitro: Film autoradiography. Adjacent AD temporal lobe sections were incubated with (A) ^{125}I-Aβ 1-40 and exposed for six days or (B) ^{125}I-PUT-Aβ 1-40 and exposed for one day. Scale bars = 5 mm.

On the basis of our finding that ^{125}I-PUT-Aβ 1-40 has a greater affinity for neuritic plaques than ^{125}I-Aβ 1-40, we next determined the effect of putrescine on binding by incubating the peptides in the absence or presence of excess unbound putrescine. If putrescine also binds to amyloid, then one might expect to see decreased binding of iodinated peptide in a competitive manner in the presence of excess unbound putrescine. Figure 4 illustrates the binding of ^{125}I-Aβ 1-40 and ^{125}I-PUT-Aβ 1-40 to amyloid deposits in vitro in the absence or presence of a 10-fold excess of unbound putrescine. There appears to be no appreciable effect on binding of iodinated peptide in the presence of unbound putrescine, even at 10-fold excess. This suggests that putrescine itself does not bind specifically to amyloid, but may enhance binding by some other mechanism.

Labeling of amyloid plaques in vivo. ^{125}I-PUT-Aβ 1-40 was then tested for its ability to cross the BBB and label amyloid deposits in vivo following intravenous injection in transgenic mice that express two mutant human proteins, APP and PS1, associated with familial AD[6]. These mice develop amyloid deposits and behavioral deficits within 12 weeks of age[6]. We found by quantitative histological analyses of amyloid deposition that deposition of neuritic-type plaques occurs at a rapid rate starting around 12 weeks, reaching an amyloid burden of over 3.5% in cortex and hippocampus in one year (unpublished data). For these experiments, two mice (27 weeks of age) were injected with 200 μg of ^{125}I-PUT-Aβ 1-40. The results are shown in Figure 5. Figure 5A illustrates a photomicrograph of a section through the medial septum that exhibits several amyloid deposits radiolabeled with ^{125}I-PUT-Aβ 1-40. This particular section was exposed for eight weeks, but labeled deposits could be observed after only one week of exposure. Figure 5B illustrates a higher magnification of one of the deposits in

Table 1. PS and V_p of Aβ 1-40 and PUT-Aβ 1-40 at the BBB

	PS[a]			V_p[b]		
	Aβ 1-40	PUT-Aβ 1-40	RI[c]	Aβ 1-40	PUT-Aβ 1-40	RI[c]
Cortex	10.9 ± 0.6	25.5 ± 3.2	2.3***	9.4 ± 0.4	13.9 ± 0.7	1.5**
Caudoputamen	12.8 ± 0.7	26.0 ± 3.4	2.0***	6.6 ± 0.4	9.2 ± 0.8	1.4**
Hippocampus	12.7 ± 1.4	24.3 ± 2.9	1.9***	8.6 ± 1.4	10.1 ± 0.5	1.2
Thalamus	13.4 ± 0.7	30.2 ± 3.2	2.3***	12.2 ± 0.6	11.1 ± 0.3	0.9
Brainstem	17.7 ± 1.2	35.1 ± 5.3	2.0***	16.2 ± 1.2	25.5 ± 1.7	1.6***
Cerebellum	18.2 ± 1.5	34.8 ± 4.1	1.9***	12.4 ± 0.8	15.1 ± 0.8	1.2

[a]PS is the permeability coefficient × surface area product ($\bar{x}$ ± s.e.m. × 10^{-6} ml g^{-1} s^{-1}; n = 10).
[b]V_p is the residual plasma volume ($\bar{x}$ ± s.e.m. in microliters per gram; n = 10).
[c]RI is the relative increase of PUT-Aβ 1-40 compared to Aβ 1-40. Analysis of variance followed by Bonferroni multiple comparisons of each PUT-Aβ vs. Aβ: *P < 0.05; **P < 0.01, ***P < 0.001.

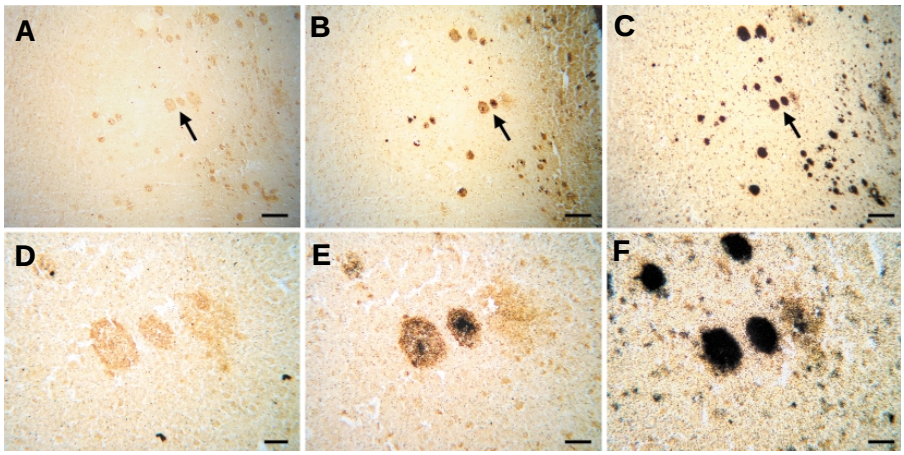

Figure 3. ^{125}I-Aβ 1-40 and ^{125}I-PUT-Aβ 1-40 labeling of amyloid deposits in vitro with equivalent radioactivity. (A-C) Adjacent sections of AD temporal lobe incubated with buffer alone (A), or 5×10^5 c.p.m. of either ^{125}I-Aβ 1-40 (B) or ^{125}I-PUT-Aβ 1-40 (C), and processed for anti-Aβ IH and emulsion autoradiography with an equal exposure time of six days. Scale bars = 200 μm. (D-F) Higher magnification of amyloid deposits indicated by arrows in A-C. Scale bars = 50 μm.

which the brown IH reaction product is visible beneath the exposed silver grains. Figure 5C illustrates the adjacent section that was stained for thioflavin S and confirms the presence and distribution of the same amyloid deposits. Radiolabeled amyloid deposits were also observed in the hippocampus and fimbria/fornix of each animal. An APP, PS1 transgenic mouse injected intravenously with 200 μg of ^{125}I-Aβ 1-40 did not exhibit labeling of any parenchymal amyloid deposits, aside from faint pial and some residual vascular labeling, with up to 12 weeks of exposure. These results demonstrate that ^{125}I-PUT-Aβ 1-40 is able to cross the BBB and bind to amyloid deposits in vivo following intravenous administration.

Discussion

Putrescine modification of Aβ 1-40 significantly increased its permeability at the BBB an average of twofold. It should be noted that the PS values for Aβ 1-40 are relatively high already and compare to that of insulin, for which the PS value in rat cortex is 15.78×10^{-6} ml g^{-1} s^{-1} and for which BBB uptake is known to occur by receptor-mediated transport[12]. As a basis for comparison, the PS value for albumin in rat cortex is 0.15×10^{-6} ml g^{-1} s^{-1}, which we believe crosses the BBB by passive diffusion[12]. Therefore, the high PS value for Aβ 1-40 coupled with stereospecific BBB permeability data for L-Aβ 1-40 suggest that the BBB transport occurs by a receptor-mediated mechanism[17,18]. The PS values for D-Aβ 1-40 are less than 1×10^{-6} ml g^{-1} s^{-1} (ref. 18). Other evidence also supports the hypothesis that the increased permeability of PUT-Aβ 1-40 may be receptor-mediated rather than by simple electrostatic mechanisms. In an earlier study, we found that modification of the antioxidant enzyme, superoxide dismutase with spermidine or spermine, which have higher charge densities than putrescine, resulted in lower permeability than with putrescine[13]. The opposite would be expected if purely electrostatic mechanisms were responsible, and therefore a polyamine transporter may be

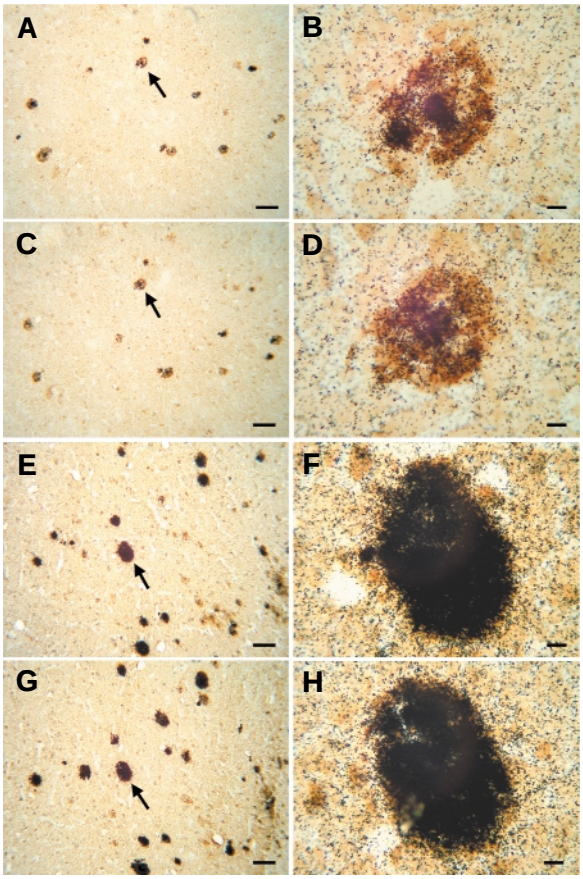

Figure 4. ^{125}I-Aβ 1-40 and ^{125}I-PUT-Aβ 1-40 labeling of amyloid deposits in vitro in the absence or presence of a 10-fold excess of unbound putrescine. (A, E) Sections of AD temporal lobe incubated with 100 pM of either ^{125}I-Aβ 1-40 (A) or ^{125}I-PUT-Aβ 1-40 (E) in the absence of unbound putrescine. (C, G) The adjacent section incubated with 100 pM of either ^{125}I-Aβ 1-40 (C) or ^{125}I-PUT-Aβ 1-40 (G) in the presence of 10-fold excess unbound putrescine. All sections were processed for anti-Aβ IH and emulsion autoradiography with an equal exposure time of six days. Scale bars (A, C, E, G) = 100 μm. (B, D, F, H) Higher magnification of amyloid deposits indicated by arrows in A, C, E, G, respectively. Scale bars = 10 μm.

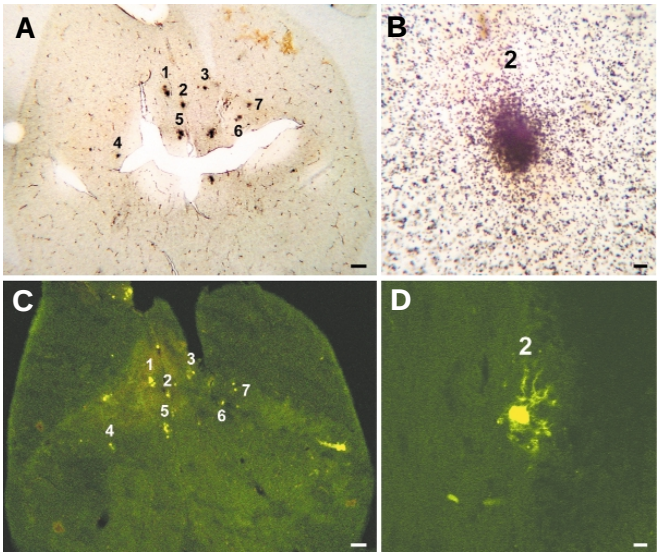

Figure 5. ^{125}I-PUT-Aβ 1-40 labeling of amyloid deposits in vivo in APP, PS1 transgenic mouse brain. (A) Section through medial septum processed for anti-Aβ IH and emulsion autoradiography with eight weeks of exposure exhibiting several labeled deposits. (C) Adjacent section showing same deposits stained with thioflavin S. (B, D) Higher magnification of deposit no. 2. Scale bars (A, C) = 100 μm; (B, D) = 10 μm.

involved[13]. A doubling of the already high PS value for Aβ 1-40 by putrescine modification, therefore, represents a marked increase in its permeability at the BBB with important physiological implications for enhanced delivery into the CNS.

In addition to having increased permeability at the BBB, ^{125}I-PUT-Aβ 1-40 also labeled amyloid deposits in vitro with greater affinity than ^{125}I-Aβ 1-40, based on shorter exposure times or increased intensity of autoradiography emulsion. There is not an obvious explanation for this, since the addition of 10-fold excess unbound putrescine did not decrease labeling in a competitive manner. Intuitively, the addition of putrescine to the structure of Aβ 1-40 could possibly block binding sites and actually reduce labeling by interference. Also, since amyloid is highly hydrophobic and PUT-Aβ 1-40 appears to be relatively less hydrophobic than Aβ 1-40, based on a shorter retention time during HPLC, one might expect to observe decreased labeling with ^{125}I-PUT-Aβ 1-40 due to decreased hydrophobicity. A possible explanation is that putrescine modification increases the β-hydro-moment at other regions of the peptide, thus increasing its affinity for amyloid deposits.

In Figure 1, the peak for PUT-Aβ 1-40 appears to be broader than that for Aβ 1-40, possibly as a result of heterogeneity of the specific amino acid residues modified with putrescine, which could possibly affect labeling. The primary sequence of Aβ 1-40 contains six amino acid residues for which the carboxylic acid groups were targeted for modification and which may or may not be modified in any combination depending on the tertiary structure and ionization state of the peptide during modification. In order to control for this, the pH was maintained at a constant level throughout the reaction and a duration of 3 h was used to achieve a steady state of modification. However, the results show that the binding of both ^{125}I-PUT-Aβ 1-40 and ^{125}I-Aβ 1-40 was specific for dense-core, neuritic-type amyloid deposits, since no diffuse deposits were labeled and background labeling was not noticeable. Also, when HPLC purification was omitted and only dialysis and preparative cartridge purification used, no specific labeling of amyloid deposits was observed in vitro. Furthermore, ^{125}I-PUT-Aβ 1-40 actually demonstrated higher affinity for the amyloid deposits based on shorter exposure times and increased exposure of autoradiography emulsion compared to ^{125}I-Aβ 1-40.

The most significant result of this study was that ^{125}I-PUT-Aβ 1-40 labeled amyloid deposits in the brains of living APP, PS1 transgenic mice. One previous experiment using aged squirrel monkeys, known to exhibit amyloid deposits with advanced age, reported labeling of amyloid deposits in brain following injection of radiolabeled Aβ 1-40 into the carotid artery[9]. It has been reported, however, that the preponderance of amyloid deposits in aged squirrel monkeys is associated with the cerebrovasculature and the few deposits found within the parenchyma tend to be diffuse rather than associated with neuritic plaques[19]. In fact, Ghilardi and coworkers[9] reported that labeling was observed only in cerebrovascular amyloid deposits, and they did not observe any parenchymal deposits, labeled or unlabeled, in their subjects.

In the present study, many parenchymal amyloid deposits were labeled while only minor cerebrovascular and pial labeling was observed. The labeled deposits were most prevalent in the dorsal hippocampus, medial septum, and fimbria/fornix. In the present study, only a few labeled deposits were observed in the cortex, which may be related to the density of vascularization. Many of the labeled deposits in the hippocampus were situated near the hippocampal fissure, which typically contains some large blood vessels. Some labeled deposits were associated with cerebrovascular amyloid, but most had no apparent relation to blood vessels, particularly those in the medial septum and fimbria/fornix. Since these results were obtained with only a single, 200 μg dose of ^{125}I-PUT-Aβ 1-40 and a duration of 4 h, higher and more frequent doses of different durations might yield more extensive labeling of amyloid deposits in the cortex.

Increased brain uptake of ^{125}I-PUT-Aβ 1-40 or ^{125}I-Aβ 1-40 and labeling might result if general disruption of the BBB occurred in APP, PS1 transgenic mice, as has been proposed by some to occur in AD[20]. Studies of APP, PS1 transgenic mice in this laboratory, however, have observed no significant alterations in BBB permeability (unpublished data). In the present study, no labeled deposits were observed after injection of ^{125}I-Aβ 1-40, even after 12 weeks of exposure, despite its relatively high BBB permeability. The presence of a receptor for Aβ 1-40 (and Aβ 1-42) at the BBB[17,18] may, therefore, allow its uptake only at the luminal surface and not at the abluminal surface of the endothelial cell. This suggests that the cerebrovascular amyloid deposition seen in AD and other dementias may have as its origin Aβ from the systemic circulation, whereas the parenchymal amyloid deposition may result from the de novo synthesis of Aβ within the brain itself. When brain uptake of ^{125}I-PUT-Aβ 1-40 and ^{125}I-Aβ 1-40 was calculated based on the radioactivity in the perfused brain compared to the total amount injected, there was 10-fold more uptake of ^{125}I-PUT-Aβ 1-40 than ^{125}I-Aβ 1-40 (0.35% vs. 0.03%, respectively). Future experiments will be performed with increased dose, duration, and frequency of injection of ^{125}I-PUT-Aβ 1-40 in an effort to attain more extensive labeling of amyloid deposits, particularly in the cortex.

Our results support the development of radiolabeled PUT-Aβ 1-40 as a marker of amyloid deposition for use as a diagnostic tool for AD in humans. Future experiments will be performed to radiolabel PUT-Aβ 1-40 with an isotope more suitable for diagnostic imaging, namely ^{123}I, and to test the ability of ^{123}I-PUT-Aβ 1-40 to label and detect amyloid deposits in vivo in APP, PS1 transgenic mice using one of the same methods of diagnostic imaging as that used in humans, single photon emission computed tomography (SPECT). Since ^{123}I has a shorter half-life than ^{125}I (13 h vs. 60 days, respectively) but higher γ-energy (159 keV vs. 35 keV, respectively), pharmacokinetic and biodistribution experiments are currently underway using ^{123}I-PUT-Aβ 1-40 and SPECT to determine the optimal dose, frequency of dosing, and duration post-dose to achieve maximum brain uptake and minimum background interference. In the event that injecting ^{123}I-PUT-Aβ 1-40 into humans is problematic, other peptides that have been shown to bind amyloid as well as inhibit deposition[21,22], or other isotopes suitable for diagnostic brain imaging techniques such as ^{18}F or ^{99m}Tc (ref. 23), could subsequently be investigated.

Experimental protocol

PS and V_p measurements of radioiodinated Aβ proteins. Permeability of Aβ 1-40 or PUT-Aβ 1-40 at the BBB was determined using an intravenous bolus injection technique that has been described in detail[10-12]. Briefly, putrescine modification of synthetic human Aβ 1-40 was first performed by covalent linkage of the polyamine to carboxylic acid groups using carbodiimide at a pH of 6.7 (refs 13,14). Next, separate aliquots of native (Aβ 1-40) or putrescine-modified (PUT-Aβ 1-40) peptides were labeled with ^{125}I or ^{131}I (Amersham, Arlington Heights, IL) using a modified chloramine-T procedure. After putrescine modification and radioiodination, PS and V_p values for the BBB permeability of Aβ 1-40 and PUT-Aβ 1-40 were then determined in normal adult male Sprague–Dawley rats (400 g, Harlan, Cincinnati, OH). All procedures performed were in accordance with NIH Guidelines for the Care and Use of Laboratory Animals. Briefly, a bolus of 0.9% NaCl containing Aβ 1-40 or PUT-Aβ 1-40 labeled with ^{125}I was injected rapidly into the catheterized brachial vein of an anesthetized rat (sodium pentobarbital, 25 mg kg^{-1}, intraperitoneally). Blood (200 μl) was sampled from the brachial artery at several intervals during the next 15 min. An aliquot of the peptide labeled with ^{131}I was then injected into the brachial vein 15 s before sacrifice of the animal to serve as a measure of residual plasma volume (V_p; in microliters per gram). Plasma samples and several brain regions were assayed for ^{125}I and ^{131}I radioactivity in a two-channel γ-counter (Cobra II, Packard). The permeability coefficient × surface area products (PS; 10^{-6} ml g^{-1} s^{-1}) for Aβ 1-40 and PUT-Aβ 1-40 were then calculated using the V_p (in microliters per gram) as a measure of residual plasma volume[10]. Statistical evaluations of PS and V_p were performed using ANOVA followed by Bonferroni multiple comparisons.

RP-HPLC purification of radioiodinated protein. For the amyloid labeling experiments, the radioiodinated Aβ 1-40 and PUT-Aβ 1-40 were purified using RP-HPLC to remove unbound ^{125}I and unlabeled peptide to achieve very high specific activity[8,9]. Following radioiodination, the peptides were dialyzed for 4 h against 0.2 M NaI and then passed over a C_{18} preparative cartridge (Sep-Pak Light, Waters, Milford, MA) to remove unbound ^{125}I. The peptide was eluted stepwise with increasing concentrations of acetonitrile (ACN) in 0.05% trifluoroacetic acid (TFA) (10, 20, 40, 80, 100% ACN, Fisher Scientific, Fair Lawn, NJ). The peptides eluted primarily in the 40 and 80% ACN fractions. The peptides were reduced with 2-mercaptoethanol (2-ME) and concentrated to 0.25 ml with a Speed Vac (Savant, Farmingdale, NY).

The ^{125}I-Aβ 1-40 and ^{125}I-PUT-Aβ 1-40 were then purified by RP-HPLC (System Gold, Beckman Instruments, Fullerton, CA) using a gradient method with a binary solvent system (buffer A, 0.05% TFA–99.95% water; buffer B, 80% ACN–0.05% TFA–19.95% water). Each peptide was injected and purified using a 1 h gradient of 0–100% buffer B at a rate of 1 ml min^{-1} using a small-bore, C_{18} column (5 μm, 4.6 × 250 mm, no. 218TP54, Vydac, Hesperia, CA). One-minute (1 ml) fractions were collected with the detector turned off so as not to quench any of the radioactivity. Aliquots (5 μl) of 10 fractions surrounding the most radioactive fraction were then counted with the γ-counter to identify the fraction with the highest radioactivity. That fraction, containing the purest ^{125}I-labeled peptide, was then concentrated to 0.25 ml with a Speed Vac to remove the ACN and stored at -20°C in the presence of 2-ME. Aliquots of the RP-HPLC fractions presumed to contain the ^{125}I-Aβ 1-40 and ^{125}I-PUT-Aβ 1-40 were analyzed by sodium dodecyl sulfate–polyacrylamide gel electrophoresis (SDS–PAGE). Only a single band was observed for all fractions of ^{125}I-Aβ 1-40 and ^{125}I-PUT-Aβ 1-40, verifying their purity (data not shown).

Labeling of amyloid plaques in vitro. The purified ^{125}I-Aβ 1-40 and ^{125}I-PUT-Aβ 1-40 were incubated with sections of unfixed AD temporal lobe cortex. Three adjacent sections were incubated with ^{125}I-Aβ 1-40, ^{125}I-PUT-Aβ 1-40, or vehicle according to published methods[8,9]. Briefly, the sections were blocked with 0.1% bovine serum albumin (BSA) in 0.05 M Tris HCl–0.9% NaCl, pH 7.0 (TBS) for 30 min. The sections were then incubated for 3 h with 100 pM ^{125}I-Aβ 1-40 or ^{125}I-PUT-Aβ 1-40, or alone in 250 μl of TBS containing 0.1% BSA, 0.6 mg ml^{-1} magnesium chloride, 0.04 mg ml^{-1} bacitracin, 0.002 mg ml^{-1} chymostatin, and 0.004 mg ml^{-1} leupeptin. After washing with TBS four times and rinsing with distilled water twice, the sections were allowed to air dry overnight in a box with desiccant at 4°C.

Immunohistochemistry and autoradiography. The sections were then subjected to IH for amyloid using an anti-Aβ monoclonal mouse antibody (4G8, Senetek, St. Louis, MO). Untreated sections were included as a positive control for antibody staining. After rehydrating with TBS, pH 7.6, the sections were fixed briefly with neutral-buffered, 10% formalin for 3 min. The sections were washed with TBS and then blocked with 1.5% normal horse serum in TBS for 30 min. The sections were incubated with the anti-Aβ primary antibody at a dilution of 1:1000 in 0.1% BSA–TBS overnight at 4°C. The primary antibody was then visualized using a Vectastain Elite ABC kit with diaminobenzidine (DAB) according to the instructions (Vector Laboratories, Burlingame, CA). The sections were allowed to air dry overnight in a box with desiccant at 4°C.

Next, the sections were exposed to high-resolution autoradiographic film (Hyperfilm MP, Amersham, Piscataway, NJ) at -70°C to visualize ^{125}I-labeled amyloid deposits. The sections were then dipped in an autoradiographic emulsion (Type NTB-3, Kodak) for direct comparison of ^{125}I-labeled amyloid deposits to anti-Aβ IH. The slides were dipped in emulsion according to the instructions and then exposed at 4°C in a lightproof box with desiccant. The slides were developed with Dektol developer and fixed according to the instructions (Kodak, Rochester, NY). The sections were dehydrated with successive changes of ethanol and xylene and then coverslipped.

Labeling of amyloid plaques in vivo. In vivo evaluations were performed using transgenic mice that express two mutant human proteins associated with familial AD and have been described in detail elsewhere[6]. Hemizygous transgenic mice (Tg2576) expressing mutant human amyloid precursor protein (APP_{695}; ref. 5) were mated with a second strain of hemizygous transgenic mice (M146L5.1) expressing mutant human PS1[6]. The animals were genotyped for the expression of both transgenes by a dot-blot method using a sample of mouse tail DNA. The mice were housed in a virus-free barrier facility under a 12 h light/dark cycle, with ad lib access to food and water. All procedures performed were in accordance with NIH Guidelines for the Care and Use of Laboratory Animals.

These APP, PS1 transgenic mice (27 weeks of age) were catheterized in the femoral vein under general anesthesia (sodium pentobarbital, 25 mg kg^{-1}, intraperitoneally) and injected with 200 μg of ^{125}I-Aβ 1-40 or ^{125}I-PUT-Aβ 1-40. One mouse was injected with ^{125}I-Aβ 1-40 and two with ^{125}I-PUT-Aβ 1-40. After 4 h, each animal was perfused with PBS and fixed with neutral-buffered, 10% formalin following an overdose with sodium pentobarbital (75 mg kg^{-1}, intraperitoneally). After cryoprotecting in 10% and 30% sucrose in PBS for 24 h each, frozen sections of each brain were cut with a freezing microtome and then processed with anti-Aβ IH and emulsion autoradiography for the presence of radiolabeled amyloid deposits using the same methods described above for the human AD brain sections.

Acknowledgments

The authors wish to thank Dr. Shirley Poduslo for her generous gift of human AD brain tissue, Dr. Karen Duff for her generous gift of PS1 transgenic mice, and Dr. John Maggio for his valuable technical advice. The authors also wish to thank Shelly Whelan for her expert technical assistance and Jennifer Scott for her expert secretarial assistance.

1. Maggio, J.E. & Mantyh, P.W. Brain amyloid—a physicochemical perspective. *Brain Pathol.* **6**, 147–162 (1996).
2. Manelli, A.M. & Puttfarcken, P.S. Beta-amyloid-induced toxicity in rat hippocampal cells: in vitro evidence for the involvement of free radicals. *Brain Res. Bull.* **38**, 569–576 (1995).
3. Weldon, D.T. et al. Fibrillar beta-amyloid induces microglial phagocytosis, expression of inducible nitric oxide synthase, and loss of a select population of neurons in the rat CNS in vivo. *J. Neurosci.* **18**, 2161–2173 (1998).
4. Selkoe, D.J. Alzheimer's disease: genotypes, phenotype, and treatments. *Science* **275**, 630–631 (1997).
5. Hsiao, K. et al. Correlative memory deficits, A-beta elevation, and amyloid plaques in transgenic mice. *Science* **274**, 99–102 (1996).
6. Holcomb, L. et al. Accelerated Alzheimer-type phenotype in transgenic mice carrying both mutant amyloid precursor protein and presenilin 1 transgenes. *Nat. Med.* **4**, 97–100 (1998).
7. Cummings, B.J. & Cotman, C.W. Image analysis of beta-amyloid load in Alzheimer's disease and relation to dementia severity. *Lancet* **346**, 1524–1528 (1995).
8. Maggio, J.E. et al. Reversible in vitro growth of Alzheimer disease beta-amyloid plaques by deposition of labeled amyloid peptide. *Proc. Natl. Acad. Sci. USA* **89**, 5462–5466 (1992).
9. Ghilardi, J.R. et al. Intra-arterial infusion of [I-125]A-beta 1-40 labels amyloid deposits in the aged primate brain in vivo. *NeuroReport* **7**, 2607–2611 (1996).
10. Poduslo, J.F. & Curran, G.L. Increased permeability across the blood–nerve barrier of albumin glycated in vitro and in vivo from patients with diabetic polyneuropathy. *Proc. Natl. Acad. Sci.USA* **89**, 2218–2222 (1992).
11. Poduslo, J.F. & Curran, G.L. Glycation increases in permeability of proteins across the blood–nerve and blood–brain barriers. *Molec. Brain Res.* **23**, 157–162 (1994).
12. Poduslo, J.F., Curran, G.L. & Berg, C.T. Macromolecular permeability across the blood–nerve and blood–brain barriers. *Proc. Natl. Acad. Sci.USA* **9**, 5705–5709 (1994).
13. Poduslo, J.F. & Curran, G.L. Polyamine modification increases the permeability of proteins at the blood–nerve and blood–brain barriers. *J. Neurochem.* **66**, 1599–1609 (1996).
14. Poduslo, J.F. & Curran, G.L. Increased permeability of superoxide dismutase at the blood–nerve and blood–brain barriers with retained enzymatic activity after covalent modification with the naturally occurring polyamine, putrescine. *J. Neurochem.* **67**, 734–741 (1996).
15. Wengenack, T.M., Curran, G.L., Olson, E.E. & Poduslo, J.F. Putrescine-modified catalase with preserved enzymatic activity exhibits increased permeability at the blood–nerve and blood–brain barriers. *Brain Res.* **767**, 128–135 (1997).
16. Poduslo, J.F., Curran, G.L. & Gill, J.S. Putrescine-modified NGF: bioactivity, pharmacokinetics, blood–brain/nerve barrier permeability, and nervous system biodistribution. *J. Neurochem.* **71**, 1651–1660 (1998).
17. Poduslo, J.F., Curran, G.L., Haggard, J.J., Biere, A.L. & Selkoe, D.J. Permeability and residual plasma volume of human, Dutch variant, and rat amyloid β-protein 1-40 at the blood–brain barrier. *Neurobiol. Dis.* **4**, 27–34 (1997).
18. Poduslo, J.F., Curran, G.L., Sanyal, B. & Selkoe, D.J. Receptor-mediated transport of human amyloid beta-protein 1-40 and 1-42 at the blood–brain barrier. *Neurobiol Dis.* **6**, 190–199 (1999).
19. Walker, L.C., Masters, C., Beyreuther, K. & Price, D.L. Amyloid in the brains of aged squirrel monkeys. *Acta Neuropathol.* **80**, 381–387 (1990).
20. Vinters, H.V. & Pardridge, W.M. The blood–brain barrier in Alzheimer's disease. *Can. J. Neurol. Sci.* **13**, 446–448 (1986).
21. Soto, C., Kindy, M.S., Baumann, M. & Frangione, B. Inhibition of Alzheimer's amyloidosis by peptides that prevent beta-sheet conformation. *Biochem. Biophys. Res. Commun.* **226**, 672–680 (1996).
22. Poduslo, J.F., Curran, G.L., Kumar, A., Frangione, B. & Soto, C. Beta-sheet breaker peptide inhibitor of Alzheimer's amyloidogenesis with increased blood–brain barrier permeability and resistance to proteolytic degradation in plasma. *J. Neurobiol.* **39**, 371–382 (1999).
23. Abbott, N.J., Chugani, D.C., Zaharchuk, G., Rosen, B.R. & Lo, E.H. Delivery of imaging agents into brain. *Advances Drug Delivery Rev.* **37**, 253–277 (1999).